Society For Biomaterials

Increased *in vivo* stability and functional lifetime of an implantable glucose sensor through platinum catalysis

Arthur E. Colvin, Hui Jiang

Sensors for Medicine and Science Inc., 20451 Seneca Meadows Parkway, Germantown, Maryland 20876-7005

Received 5 June 2012; revised 20 August 2012; accepted 21 August 2012
Published online 15 October 2012 in Wiley Online Library (wileyonlinelibrary.com). DOI: 10.1002/jbm.a.34424

Abstract: Understanding and improving *in vivo* materials related to signal stability and preservation for active chemical sensor and biosensor transduction systems is critical in achieving implantable medical sensors for long-term *in vivo* applications. During human *in vivo* clinical testing of an implantable glucose sensor based on a glucose sensitive hydrogel, post-explant analysis showed that the boronate recognition element had been oxidized from the fluorescent indicator, causing a rapid loss of signal within hours after implant. Additional wet-bench analytical evidence and reproduction *in vitro* suggests reactive oxygen species, particularly hydrogen peroxide (H_2O_2), stemming from natural inflammatory response to the material, to be the cause of the observed oxidative de-boronation. A 3-nm thick deposition of metallic platinum (Pt) placed by plasma sputtering onto the porous surface of the hydrogel, showed immediate protection from sensor signal loss due to oxidation both *in vitro* and *in vivo*, greatly extending the useful lifetime of the implantable glucose sensor from 1 day to an expected $\geq$6 months. This finding may represent a new strategy to protect an implanted material and/or device from *in vivo* oxidative damage, leading to much improved overall stability and reliability for long-term applications. © 2012 Wiley Periodicals, Inc. J Biomed Mater Res Part A: 101A: 1274–1282, 2013.

Key Words: catalytic protection with platinum, oxidation *in vivo*, reactive oxygen species, inflammatory response, implantable glucose sensor

How to cite this article: Colvin AE, Jiang H. 2013. Increased *in vivo* stability and functional lifetime of an implantable glucose sensor through platinum catalysis. J Biomed Mater Res Part A 2013:101A:1274–1282.

INTRODUCTION

For those with type I diabetes, the ongoing development of continuous glucose monitoring (CGM) technology holds great promise for improved blood glucose control. A number of development stage CGM systems have been reported over the decades to provide at least some level of uninterrupted continuous *in vivo* glucose monitoring over time periods of hours or days.[1–4] Achieving a next level of extended *in vivo* sensor operation for intervals of months or years in humans must overcome some significant engineering and materials challenges, including the protection of highly sensitive signal transduction chemistry from *in vivo* oxidation due to natural inflammatory response.[5–7] Published work aimed at protecting implantable devices and materials from *in vivo* oxidative damage has most often included use of antioxidants.[8–10] In such cases where some level of efficacy has been demonstrated, the device or material must either include or leach a drug or substance into the local *in vivo* environment, causing the device itself to become a drug delivery mechanism in addition to its original intended purpose. Adding in this additional substance release feature may add complexity, variability, and uncertainty into an implant design and may complicate proving the safety and efficacy of the device or material. In addition, because the inflammatory response is a normal part of healing that serves to kill any bacteria that may be in the wound, drugs or leached reagents which may disable this otherwise normal aspect of wound healing might compromise the patient.

Herein we report a unique, device level, materials-based, catalytic strategy to mediate the biological protection benefit from normal *in vivo* oxidative inflammatory response with the practical need to protect the performance and integrity of a glucose sensitive material used within an implantable glucose sensor, thereby greatly extending the sensor's useful lifetime in humans from 1 day to an expected $\geq$6 months.

The study device reported herein is an investigational device limited to investigational use only.
Conflict of interest: Both authors are full time employees of SMSI with equity options as a part of overall compensation. Both authors are listed as the inventors for US and international patent applications filed regarding the work reported herein. A.E. Colvin is the inventor of the SMSI core technology with all rights assigned to SMSI.
Correspondence to: A. E. Colvin; e-mail: aec@s4ms.com
Contract grant sponsors: SMSI and the research reported herein is funded by a consortium of private venture capital firms (listed on SMSI website: www.s4ms.com/about_investors.htm) and the Juvenile Diabetes Research Foundation (JDRF)

MATERIALS AND METHODS

Hydroxyethylmethacrylate (HEMA) was purchased from Polysciences, 2,2′-azobis[2-(2-imidazolin-2-yl)propane]dihydrochloride (VAZO) from Wako Pure Chemical Industries, polyethylene glycol diacrylate (PEGDA, Mn $\sim$ 700), glucose, Gibbs' reagent, Alizarin Red S, 30% hydrogen peroxide and bovine serum albumin (BSA) from Sigma, and BDH water and Xylenol Orange (XO) assay kit for hydrogen peroxide from VWR. PBS buffer and glucose indicator monomers were prepared in house.

The glucose sensitive material (indicator graft) was prepared as a phase separated, cross-linked, hydrogel copolymer from HEMA (94.3 mol %), PEGDA (5.6 mol %, cross-linker), glucose indicator monomer (0.1 mol %), VAZO (initiator), and BDH water (70 vol %), polymerized at 60°C for 3 h. To obtain the Scanning Electron Microscope (SEM) micrograph of the indicator graft on the sensor encasement, the sample was pretreated by critical point drying to preserve the porous gel structure, and coated with gold for high vacuum mode SEM imaging with a Carl Zeiss EVO40 microscope.

Platinum from a 99.99% purity target was deposited using an Electron Microscopy Sciences (EMS) 150TS sputter coater. Samples were placed on a rotating stage, and the coating chamber was evacuated to $<$0.005 mbar and backfilled with argon gas to 0.01 mbar. The current was set at 25 mA, and the coating thickness was determined by a thickness monitor mounted within the chamber.

The XO assay for hydrogen peroxide was performed according to the manufacturer's procedure. UV–visible absorption spectra were recorded with a Hewlett Packard 8453 spectrophotometer. Fluorescence spectra were obtained with a RF-5301PC spectrofluorophotometer from Shimadzu. The excitation wavelength was 380 nm, and the emission was scanned from 390 nm to 600 nm. For characterization of platinum coated sensor cores, SEM micrographs were obtained with a FEI Quanta 200ESEM in the low vacuum mode (90 Pa) with a Large Field Detector. X-ray Photoelectron Spectroscopy (XPS) and Inductively Coupled Plasma Optical Emission Spectrometry (ICP-OES) analyses were performed by a contractor. For XPS, the sample was irradiated by a low energy (1486.6 eV) monochromatic aluminum Kα X-ray, and the elemental survey spectra covered the binding energy range from 0 to 1100 eV, with a step size of 0.5 eV. For ICP-OES, platinum was extracted from samples by known volume of aqua regia and analyzed against standard solutions with known concentrations.

For sensors, noise compensated glucose signal is taken directly from the system telemetry, whereas for *in vitro* sensor test cores, glucose modulation was determined by the measured fluorescence spectra in 0 m*M* and 18 m*M* glucose solutions. The %Modulation was defined as $(I_{18\ mM} - I_{0\ mM})/I_{0\ mM}$, where $I_{18\ mM}$ is the fluorescence signal for 18 m*M* glucose, and $I_{0\ mM}$ for 0 m*M* glucose.

All work involving animals was conducted in accordance with NIH guidelines for the care and use of laboratory animals (NIH Publication #85-23 Rev. 1985) and institutional guidelines for each study site. Human clinical studies were conducted under an Investigational Device Exemption (IDE) from FDA with IRB approvals, and IRB approvals only for nonsignificant risk studies. All subjects enrolled in this research have responded to an Informed Consent which has been approved by the Institutional Committee on Human Research for each study site, and the protocol has been found acceptable by them.

RESULTS AND DISCUSSION

The SMSI glucose sensor

The Sensors for Medicine and Science (SMSI) implantable, continuous glucose sensor, currently in advanced stages of development, measures glucose concentration from the interstitial fluid (ISF) directly via fluorescence from a glucose sensitive hydrogel copolymer that is grafted onto the sensor poly-methylmethacrylate (PMMA) surface to remain in equilibrium with ambient glucose. The sensor used in this study may be characterized as a highly miniaturized, single wavelength, dual channel, wireless, microfluorimeter [Fig. 1(a)]. The sensor is configured as a small capsule-shape implant placed into the subcutaneous space of the dorsal wrist area of the arm [Fig. 1(b)]. An external reader, constructed as a wristwatch, provides wireless power, signal data telemetry, signal processing, user display, and data storage [Fig. 1(b,c)].

The system calculates a blood equivalent glucose value from real time ISF measurements made using a modulated fluorescent glucose sensitive hydrogel with a bis-boronate glucose recognition structure [Fig. 1(d,e)]. In operation, glucose diffuses from the ISF into this highly porous hydrogel matrix grafted by sequential interpenetrating network onto the surface of the sensor's PMMA encasement, where it reversibly binds to boronate, and modulates the fluorescence of the surface matrix [Fig. 1(d–f)].

Every 2 min, the external reader powers up the sensor by means of an inductive link. On power-up, the LED source is energized for approximately 30 ms to excite the fluorescent indicator [Fig. 1(c,e)]. The resultant glucose-proportional fluorescent emission pulse is detected through a pair of band-pass filtered photodiodes, and electronically encoded. This encoded signal is superimposed onto the inductive power link between the external watch reader and sensor implant, resulting in a wireless signal data transfer. The signal from the sensor is then decoded within the reader, processed, and converted to glucose values by means of an interpretive algorithm [Fig. 1(c)].

SMSI glucose sensor *in vivo* signal loss and protection strategy

Preclinical safety and efficacy studies have been conducted in rat, dog, pig, and monkey for continuous implant periods of up to 6 months with relatively minor and predictable first order signal loss kinetics over time, attributed to oxidation via low level foreign body response and photobleaching. This report pertains to the first in human studies conducted in the US under an IDE from FDA.

After IRB approvals, eleven sensors were implanted in the subcutaneous space of the dorsal wrist area of 11

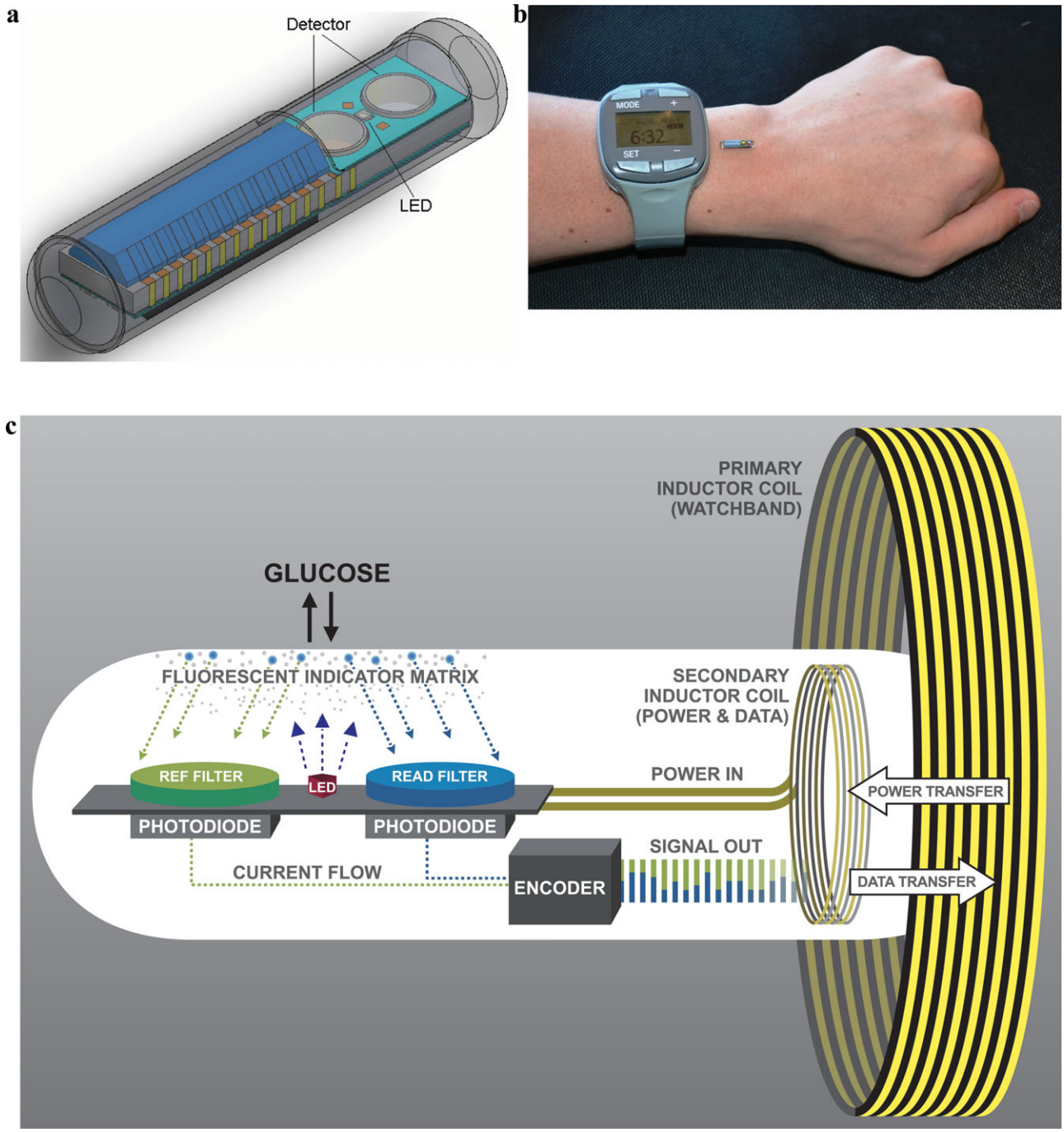

FIGURE 1. SMSI glucose sensor system. (a and b) A wireless miniature implantable glucose sensor and reader platform. (c) Working configuration of SMSI sensor system. (d and e) The fluorescent polymer indictor graft for glucose sensing with a bis-boronate glucose recognition structure. (f) Scanning Electron Microscope (SEM) micrograph of the porous indicator graft on the sensor encasement. Scale bar: 5 μm.

human type I diabetic volunteers. Surprisingly, sensors began to rapidly lose fluorescence signal within hours of implantation and many lost 90–100% of their signal within the first 24 h as shown for two examples in Figure 2(a), in strong contrast with animal implants tested for periods of up to 6 months.

Sensors that had lost 100% of their fluorescence signal were explanted to determine the cause of the unexpected rapid signal loss. From previous wet-bench analysis on much slower signal loss examples observed in animals, the boronate recognition element of the sensor indicator had been shown to be oxidized to a hydroxyl [Fig. 2(b)]. All other aspects of the molecular structure remained intact and unaltered. This site specific oxidative de-boronation was determined using Gibbs' reagent (2,6-dichloroquinone-4-chloroimide) which reacts selectively with certain

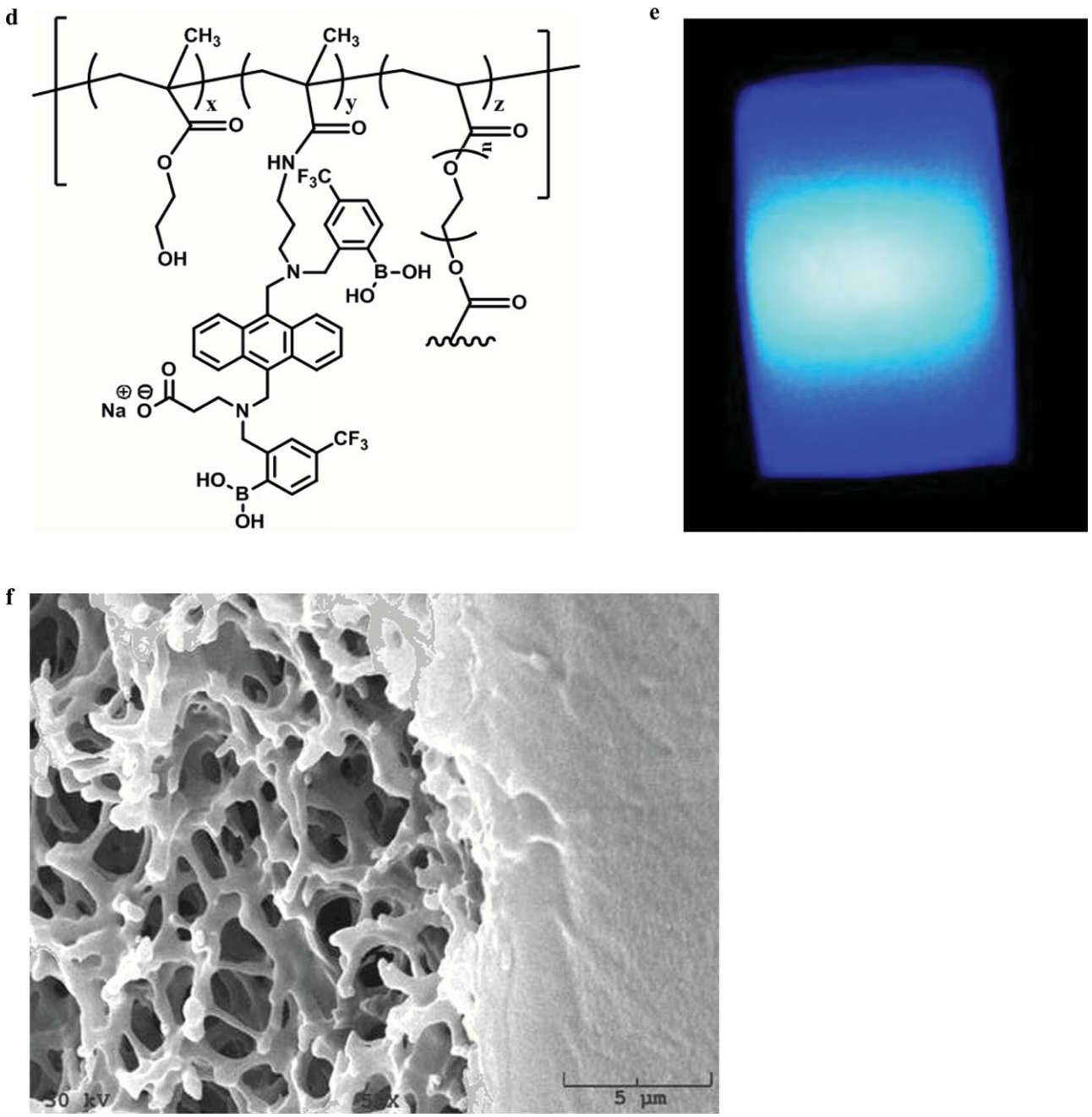

FIGURE 1. (Continued)

hydroxy-aromatic compounds (i.e. phenols and naphthols).[11] A positive test indicates the presence of a simple alkyl phenol.[12] Indicator samples removed from animals after long periods of implantation (months) were positive for phenol on treatment with Gibbs' reagent, whereas *in vitro* control samples stored in PBS were negative, thus confirming that phenolic moieties were present within the explanted indicator matrix. A UV–vis absorption peak indicating a methylphenol group was also observed with Gibbs' treated explanted samples along with a Gibbs' treated 2-methylphenol control.

We hypothesized this oxidative de-boronation to be the same reaction observed now in humans, but at a much faster rate than previously measured from all animals. Indeed, quantitative analysis for boronic acids titrated against Alizarin Red S,[13,14] a dye that binds strongly to boronic acids, indicated a greater than 70% loss of boronate from human explanted sensors relative to *in vitro* controls.

That boronate can be selectively oxidized from within the overall molecular structure of the indicator is consistent with relative bond energies published by Hall where C—B

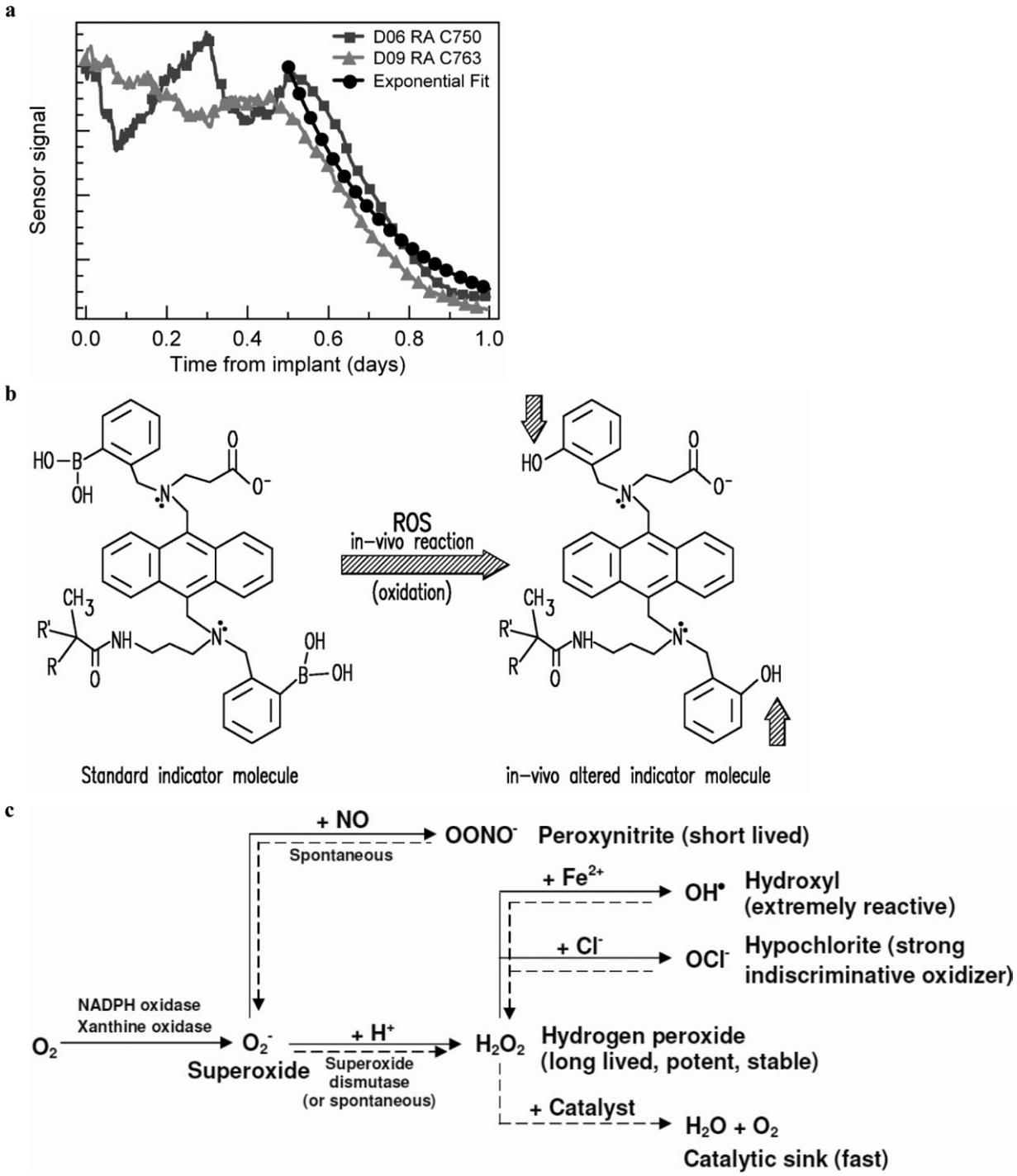

FIGURE 2. SMSI glucose sensor degradation and protection strategy *in vivo*. (a) Exemplary rapid sensor signal loss from diabetes patient D06 (right arm, sensor C750) and D09 (right arm, sensor C763). The exponential fit was calculated based on a single-exponential decay model. (b) Oxidative de-boronation reaction *in vivo* by ROS for the indicator molecule. (c) ROS generation and protection strategy *in vivo*.

bonds are the lowest energy within the structure at 323 kJ/mol, followed by C—C bonds at 358 kJ/mol and the much stronger B—O bonds at 519 kJ/mol.[15]

From natural wound healing response, neutrophils are temporally coincident with the rapid signal loss period observed in humans,[5] suggesting that neutrophil generated reactive oxygen species (ROS), especially H_2O_2, from natural inflammatory response,[16–19] may be responsible for the fast *in vivo* oxidative de-boronation. Both superoxide anion (O_2^-) and hydrogen peroxide are directly associated mediators of inflammation.[5] Superoxide is rapidly converted *in vivo* to hydrogen peroxide and water by superoxide dismutase[17,18] [Fig. 2(c)]. Additional *in vitro* treatment of indicator monomer with H_2O_2 in PBS monitored by high-performance

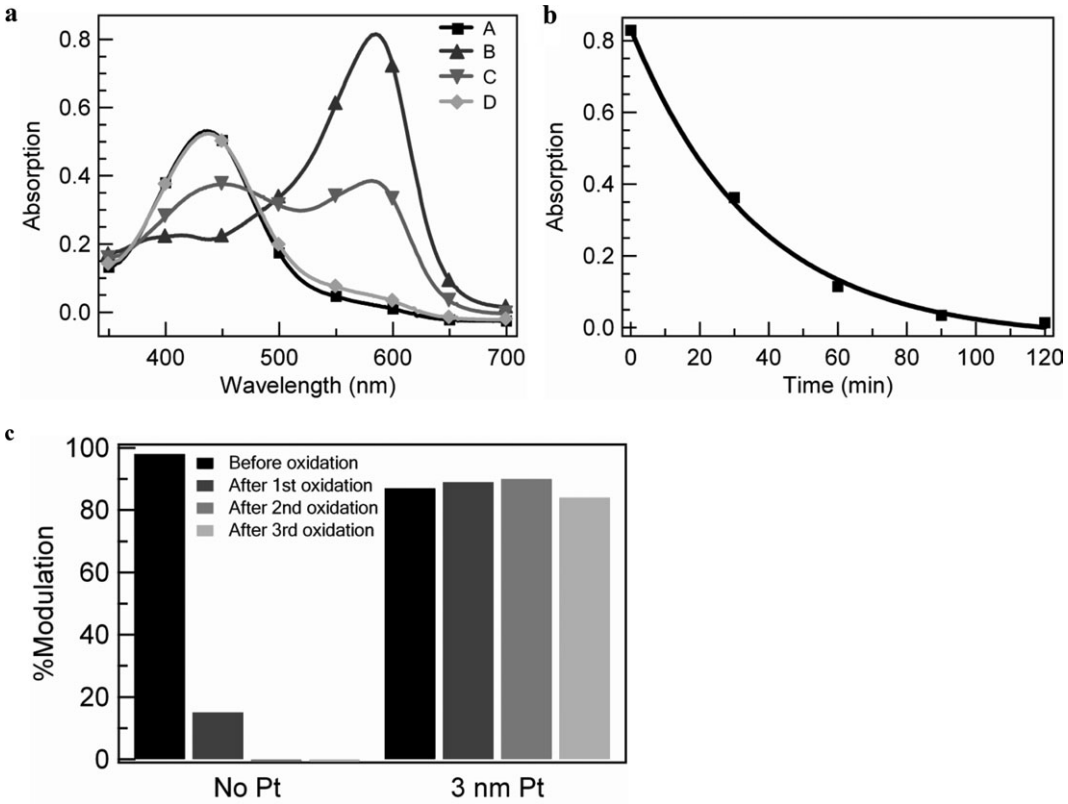

FIGURE 3. Platinum protection against H_2O_2 *in vitro*. (a) Absorption of XO assay solution A (no H_2O_2), B (200 μ*M* H_2O_2), C (B with Pt sample for 30 min), and D (B with Pt sample for 90 min). (b) Kinetic curve for H_2O_2 decomposition measured by absorption at 586 nm. (c) %Modulation measured before and after oxidation cycle for sensor graft without and with 3 nm Pt.

liquid chromatography and mass spectrometry confirmed that both mono and bis de-boronated phenolic species were the major products.

Our goal then became to develop a self protecting material means to prevent indicator oxidation from ambient ROS, especially H_2O_2, and the strategy was to use a catalyst [Fig. 2(c)]: trapping and sinking H_2O_2 directly by catalysis, and O_2^- indirectly by induction, and in turn, starving other ROS such as $OONO^-$, $OH^\bullet$, and OCl^- from essential precursors.

Platinum catalysis against hydrogen peroxide *in vitro*

For hydrogen peroxide, it is well known that silver,[20] palladium,[21,22] platinum,[22] manganese dioxide,[23] and silver oxide,[24] can catalyze decomposition to water and oxygen. An *in vitro* test using fine platinum mesh wrapping a sensor core (sensor without optoelectronics inside) and submerged into 200 μ*M* hydrogen peroxide solution at 37°C for 24 h completely protected the core from oxidation. Adding in physiological levels of protein did not show any inhibition of the catalyst. Studies reported by the FDA (www.fda.gov/MedicalDevices/ProductsandMedicalProcedures/ImplantsandProsthetics/BreastImplants/UCM064040) and others have found no evidence of metallic platinum toxicity *in vivo*.[25] Therefore, platinum was selected as a catalyst for further investigation.

Sputter coating with argon plasma is a typical process used to deposit thin layers of metal for electron microscopy imaging that can preserve surface morphology and porosity of the substrate. Using an EMS 150TS coater, configured with a platinum target and a film thickness monitor, we applied a very thin layer (1 nm or 3 nm) of platinum metal to the outer surface of our 100 μm thick porous hydrogel indicator graft, producing a porous catalyst layer, through which hydrogen peroxide must then diffuse to access the indicator molecules within the graft.

Based on the exemplary *in vivo* sensor signal loss profiles [Fig. 2(a)], and *in vitro* sensor signal degradation profiles measured from different concentrations of hydrogen peroxide exposure, the maximum transient concentration of hydrogen peroxide generated *in vivo* was estimated to be about 160 μ*M*. From these same *in vivo* signal loss kinetic profiles, the rate of hydrogen peroxide generation *in vivo* was estimated to be several times slower than the rate of peroxide decomposition by even a 1-nm thick platinum coating.

To standardize the process, a sensor core was sputter coated with 3 nm thick platinum. When the sample was incubated with 1 mL of 200 μ*M* hydrogen peroxide solution in PBS buffer (pH 7.4), the hydrogen peroxide concentration showed a steady decline as determined by a XO assay [Fig. 3(a)]. Without hydrogen peroxide, the assay solution remains yellow with an absorption peak at 436 nm (curve A). In the presence of 200 μ*M* hydrogen peroxide, the assay solution begins as deep purple, with an absorption peak at

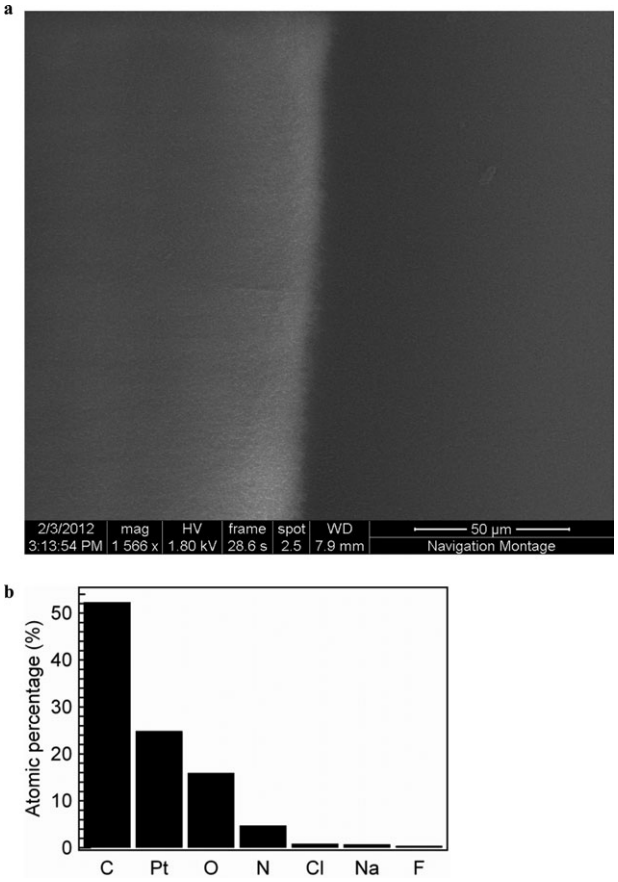

FIGURE 4. Platinum coating characterization. (a) SEM micrograph of the graft surface coated with 3 nm Pt with a mask. Scale bar: 50 μm. (b) Atomic percentage of elements detected by XPS on a 3-nm Pt coated sensor graft.

586 nm (curve B). By 90 min in the presence of the Pt sample, hydrogen peroxide was almost completely decomposed, and the assay solution resembles the control sample without hydrogen peroxide (yellow, curve D). More tests indicated that the rate of peroxide decomposition by platinum was unaffected by physiological level of proteins, using BSA as a model.

By plotting the absorption values at 586 nm versus time, the kinetic curve for hydrogen peroxide decomposition was obtained as shown in Figure 3(b). Because the absorption values are directly correlated with hydrogen peroxide concentrations, this curve shows that the decomposition reaction catalyzed by platinum coating is first order with respect to hydrogen peroxide, with a rate constant of 5.7×10^{-4} s^{-1}, which is about an order of magnitude faster than the *in vivo* sensor signal degradation rate constant estimated by a single-exponential fit [Fig. 2(a), 4.7×10^{-5} s^{-1}].

Because the sputtered platinum on the graft surface decomposes hydrogen peroxide quickly at physiological levels, it should also protect the indicator from being damaged by hydrogen peroxide. Indeed, as shown in Figure 3(c), without platinum, a sensor graft was damaged after only one oxidation cycle (200 μ*M* hydrogen peroxide, 37°C, 24 h), indicated by the dramatic loss in glucose modulation from 98% to 15% (%Modulation = $(I_{18\ mM} - I_{0\ mM})/I_{0\ mM}$, where $I_{18\ mM}$ is the fluorescence signal for 18 m*M* glucose, and $I_{0\ mM}$ for 0 m*M* glucose). However, with surface sputtered platinum, a sensor graft survived three oxidation cycles without any noticeable signal modulation loss.

Overall, platinum coating did not adversely influence sensor performance in any respect during *in vitro* tests, likely due to the negligible platinum thickness (3 nm) relative to the overall porous morphology and thickness of the graft layer (about 100 μm).

Platinum coated sensor graft characterization

The platinum coated sensor graft was further characterized before *in vivo* testing. A graft surface was coated with platinum using a mask so that only half of the graft would be coated at 3 nm thick, and then imaged with SEM. As shown in Figure 4(a), there is a clear line between the uncoated (left) and Pt coated (right) areas, and as expected, no morphological difference is noted between the two halves. Overall, the platinum coating looks very uniform even though it is only 3 nm thick, consistent with the excellent protection effect observed *in vitro*.

The nominal 3 nm thickness and composition of platinum on the graft surface was confirmed by XPS and ICP-OES. With XPS, the only other metal detected besides Pt, was Na, coming from the PBS buffer from which the sensor core was dried. Based on the surface elemental composition [Fig. 4(b)] observed with XPS, and an assumption of an inelastic mean free path of 15 nm for photoelectrons, a multilayered model for Pt thickness estimation was built. The coating thickness was estimated to be likely 3.6 nm (between 3.0 nm and 4.5 nm), and is consistent with the nominal value. With ICP-OES, the weight of Pt on a sensor core was determined. On average, each sensor core measured about 4.9 μg platinum, well within in the range of expected weight for a 3-nm thick coating.

SMSI glucose sensor protection *in vivo*

After additional toxicity studies to confirm the safety of the catalyst, a second clinical study was conducted to evaluate the effectiveness of a 3-nm platinum layer to protect the sensor from *in vivo* oxidation in humans as was observed in the first trial. In this study, 21 sensors were sputter coated with 3 nm platinum. Twelve sensors were prepared as uncoated controls. After IRB approval, all sensors were implanted into the subcutaneous space of the right or left arm dorsal wrist area of type 1 diabetes volunteers. In both the Pt group, and the control group, sensors were implanted into both arms designated in Table I as "RA" or "LA" as right arm or left arm respectively for each subject.

Signal profiles from four subjects representing the extremes of signal degradation with and without platinum from both clinical trials are shown in Figure 5(a), and the overall composite data from all subjects is shown in Table I and Figure 5(b).

In Figure 5(a), the signals for C750 (D06 RA) and C763 (D09 RA) without platinum coating are extensions of the data shown in Figure 2(a), which only show the signal

TABLE I. Comparison of Remaining Modulation for Sensors Without (12 sensors) and with (21 sensors) 3 nm Pt

No Pt	Sensor Lot #	Modulation Remaining at Day 28 After Implant (%)	3 nm Pt	Sensor Lot #	Modulation Remaining at Day 29 After Implant (%)
D05 LA	03052011	18	D18 LA	05202011	88
D05 RA	03252011	0	D18 RA	05202011	85
D06 LA	03052011	52	D19 LA	05202011	74
D06 RA	03252011	0	D19 RA	05202011	73
D07 LA	03052011	48	D20 LA	05202011	65
D07 RA	03252011	22	D21 RA	05202011	77
D08 LA	03052011	30	D22 LA	05202011	75
D08 RA	03252011	20	D23 LA	06032011	82
D09 LA	03052011	48	D23 RA	05202011	60
D09 RA	03252011	0	D24 LA	06032011	84
D10 RA	03252011	40	D24 RA	05202011	60
D11 LA	03252011	0	D25 LA	06032011	74
			D25 RA	05202011	74
			D26 LA	06032011	88
			D26 RA	06032011	88
			D27 LA	07222011	88
			D27 RA	07222011	84
			D28 LA	07222011	64
			D28 RA	07222011	85
			D29 LA	07222011	88
			D29 RA	07222011	83
Combined		23 ± 20			78 ± 9

within the first day. As noted previously, the signal for these sensors without platinum drops to near zero within the first day, indicating that the fluorescent indicator has been completely oxidized. On the contrary, platinum sputtered sensors C975 and C997 did not show any large signal loss during the entire month of implant time.

Figure 5(b) presents the comparative results from all the *in vivo* implants from both studies as shown in Table I. It shows the average remaining modulation (relative to initial glucose modulation before implant), as well as associated standard deviation, for the sensors on day 28 (no Pt, 12 sensors) or 29 (with Pt, 21 sensors) after implant. As can be seen from the data, the platinum coating preserves signal (in terms of average glucose modulation remaining) relative to the untreated devices by a factor of almost fourfold. More importantly, no sensors with platinum coating are degraded to zero as is typical within the control group. Also, the significant sensor-to-sensor and/or subject-to-subject variability in remaining modulation (in terms of standard deviation) displayed in the control group is not seen in the platinum coated group (i.e., much smaller standard deviation). The data clearly indicates that platinum is providing local protection of the indicator system within the microenvironment of the graft in humans.

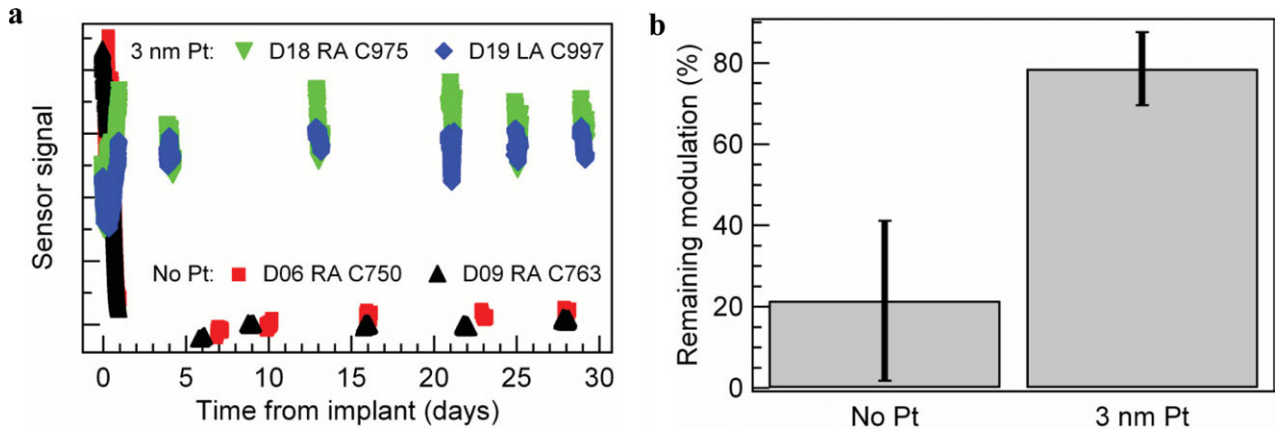

FIGURE 5. Platinum protection *in vivo*. (a) Exemplary sensor signal from diabetes patient for sensors without (D06, right arm, C750, and D09, right arm, C763) and with (D18, right arm, C975, and D19, left arm, C997) 3 nm Pt. (b) Remaining modulation for sensors without (12 sensors) and with (21 sensors) 3 nm Pt. Error bar shows the standard deviation. [Color figure can be viewed in the online issue, which is available at wileyonlinelibrary.com.]

Using a nanoparticulate catalyst to protect the material against *in vivo* ROS-driven oxidation appears to have several distinct advantages over reagent leach and drug based strategies. First, the protective catalyst remains integral to the material surface at full potency, appears safe, and does not dissipate over time. Platinum coated sensors explanted from humans after 1 month remained equally potent in degrading hydrogen peroxide when retested *in vitro*. Second, the very small amount of platinum required does not affect the performance of the sensor. Although platinum is expensive, the tiny quantity used is inexpensive and easy to install by plasma sputtering. Lastly, ROS sinking is limited to the localized microenvironment of the device itself so as to not compromise or inhibit physiological defenses through oxidation reactions that are necessary for general protection and healthy wound healing. Although the current results were obtained from glucose sensing material on SMSI sensors, we believe that a similar protection strategy may be applicable to other implanted devices and materials for *in vivo* applications.

CONCLUSIONS

Our observations and wet-bench analysis show that rapid signal loss from implanted glucose sensors observed during human trials was due to loss of the boronate recognition moiety from the indicator molecule by oxidation. Without the boronate moiety, the reversible indicator cannot bond with glucose, and modulation becomes impossible. Because of the signal loss kinetics within the first 24 h, and within the context of the observation, we came to suspect neutrophils, acting within a normal inflammatory response to the implant, to be the most likely source of ROS involved. *In vitro* modeling reactions and reaction product analysis indicated hydrogen peroxide to be the most likely ROS species produced by neutrophil that is directly responsible for the *in vivo* oxidation resulting in loss of signal within 1 day. Sensors that were subsequently implanted with a 3-nm thick layer of metallic platinum as a catalyst were all protected from rapid signal loss throughout the implant period of 29 days, with approximately 80% of their modulation (on average) remaining at the time of explant, greatly extending the sensor's operational lifetime in humans. We believe that this work demonstrates a potentially new design strategy for protecting a susceptible implant device and/or material against oxidative stress for long-term chemical and mechanical stability.

ACKNOWLEDGMENTS

The authors acknowledge the assistance and expertise of Michael McCaffery (Director) and The Integrated Imaging Center at The Johns Hopkins University, and Kathy Lowe of The Morphology Laboratory at The Virginia Polytechnic Institute and State University for SEM imaging. We wish to thank Dan Ferraro for his invaluable mechanical design, fabrication, and modeling, Taylor Colvin for photography, Jason Embrey for graphics help, and Drs. Mark Mortellaro, Carrie Lorenz, and Xiaolin Wang for their analytical chemistry and numerical analysis contributions respectively, and Mr. Steve Walters for clinical study management.

REFERENCES

1. Henning T. Commercially available continuous glucose monitoring systems. Chem Anal 2010;174:113–156.
2. Newman JD, Turner APF. Home blood glucose biosensors: A commercial perspective. Biosens Bioelectron 2005;20:2435–2453.
3. Garg SK. The future of continuous glucose monitoring. Diabetes Technol Ther 2009;11:S1–S3.
4. Brauker J. Continuous glucose sensing: Future technology developments. Diabetes Technol Ther 2009;11:S25–S36.
5. Anderson JM. Biological responses to materials. Annu Rev Mater Res 2001;31:81–110.
6. Sutherland K, Mahoney JR, Coury AJ, Eaton JW. Degradation of biomaterials by phagocyte-derived oxidants. J Clin Invest 1993;92: 2360–2367.
7. Anderson JM, Rodriguez A, Chang DT. Foreign body reaction to biomaterials. Semin Immunol 2008;20:86–100.
8. Baskin SI, Salem H, editors. Oxidants, Antioxidants, and Free Radicals. Washington, DC: Taylor & Francis; 1997.
9. Anderson JM, Hiltner A, Wiggins MJ, Schubert MA, Collier TO, Kao WJ, Mathur AB. Recent advances in biomedical polyurethane biostability and biodegradation. Polym Int 1998;46:163–171.
10. Bracco P, Oral E. Vitamin E-stabilized UHMWPE for total joint implants. Clin Orthop Relat Res 2011;469:2286–2293.
11. Quintana MG, Didion C, Dalton H. Colorimetric method for a rapid detection of oxygenated aromatic biotransformation products. Biotechnol Tech 1997;11:585–587.
12. Negrete-Raymond AC, Weder B, Wackett LP. Catabolism of arylboronic acids by *Arthrobacter nicotinovorans* strain PBA. Appl Environ Microbiol 2003;69:4263–4267.
13. Springsteen G, Wang B. Alizarin Red S. as a general optical reporter for studying the binding of boronic acids with carbohydrates. Chem Commun 2001; 1608–1609.
14. Springsteen G, Wang B. A detailed examination of boronic acid–diol complexation. Tetrahedron 2002;58:5291–5300.
15. Hall DG. Structure, properties, and preparation of boronic acid derivatives. Overview of their reactions and applications. In: Hall DG, editor. Boronic Acids: Preparation and Applications in Organic Synthesis and Medicine. Weinheim: Wiley-VCH; 2005, p 1–99.
16. Mantovani A, Cassatella MA, Costantini C, Jaillon S. Neutrophils in the activation and regulation of innate and adaptive immunity. Nat Rev Immunol 2011;11:519–531.
17. Kanta J. The role of hydrogen peroxide and other reactive oxygen species in wound healing. Acta Med (Hradec Králové) 2011;54: 97–101.
18. Freitas M, Lima JLFC, Fernandes E. Optical probes for detection and quantification of neutrophils' oxidative burst. A review. Anal Chim Acta 2009;649:8–23.
19. Dale DC, Boxer L, Liles WC. The phagocytes: Neutrophils and monocytes. Blood 2008;112:935–945.
20. Joksimovic-Tjapkin S, Delic D. Kinetics of concentrated hydrogen peroxide decomposition on a rotating disk. Ind Eng Chem Fundam 1973;12:33–39.
21. Bianchi G, Mazza F, Mussini T. Catalytic decomposition of acid hydrogen peroxide solutions on platinum, iridium, palladium, and gold surfaces. Electrochim Acta 1962;7:457–473.
22. McKee DW. Catalytic decomposition of hydrogen peroxide by metals and alloys of the platinum group. J Catal 1969;14:355–364.
23. Broughton B, Wentworth RL. Mechanism of decomposition of hydrogen peroxide solutions with manganese dioxide. J Am Chem Soc 1947;69:741–744.
24. Onuchukwu AI. The chemo-catalytic activity of metal/mixed metal oxides on hydrogen peroxide decomposition. Mater Chem Phys 1990;25:331–337.
25. Brook MA. Platinum in silicone breast implants. Biomaterials 2006;27:3274–3286.